frontiers | Frontiers in Materials

TYPE Original Research
PUBLISHED 01 May 2024
DOI 10.3389/fmats.2024.1406583

OPEN ACCESS

EDITED BY
Tushar Kanti Das,
Silesian University of Technology, Poland

REVIEWED BY
Suman Basak,
Dyson, United Kingdom
Sayan Ganguly,
University of Waterloo, Canada
Muhammad Danish Ali,
Silesian University of Technology, Poland

*CORRESPONDENCE
Libin He,
cungui5@163.com

RECEIVED 25 March 2024
ACCEPTED 16 April 2024
PUBLISHED 01 May 2024

CITATION
Lu Y, Gu J, Yuan J, Wu L, Wang X, Xu X, Ye F and He L (2024), Optimization of preparation techniques for high-temperature resistant waterborne phenolic-epoxy resin emulsion under low carbon background.
Front. Mater. 11:1406583.
doi: 10.3389/fmats.2024.1406583

Optimization of preparation techniques for high-temperature resistant waterborne phenolic-epoxy resin emulsion under low carbon background

Yu Lu, Jing Gu, Jinhe Yuan, Lina Wu, Xinxin Wang, Xiaofang Xu, Fuqiang Ye and Libin He*

Suzhou Paint-key Material Technology Co., Ltd, Suzhou, China

In light of escalating global climate change concerns and the pressing need to address industries with high carbon emissions and pollution, enhancing the preparation of phenol-formaldehyde epoxy resins has emerged as a critical research focus. This study seeks to fabricate waterborne phenol-formaldehyde epoxy resins with superior performance by investigating pivotal factors influencing their properties and refining preparation methods. Utilizing tetrabutylammonium bromide as a phase transfer catalyst, the phenol-formaldehyde epoxy resins are synthesized via a two-step alkalization process. Subsequent etherification reactions involve modifying the phenol-formaldehyde epoxy resins using cationic modifier diethanolamine (DEA) and anionic modifier sodium p-amino benzenesulfonate, resulting in waterborne phenol-formaldehyde epoxy resins. Subsequently, *in situ* synthesis is employed to produce nanoscale silica (SiO_2) modified waterborne phenol-formaldehyde epoxy resins. The findings reveal that when the ratio of n1 to n2 falls within the range of 1/3.25 to 1/3, the emulsion displays a moderate particle size and maintains stable storage. Furthermore, an increase in DEA dosage leads to a particle size of less than 324 nm when the ratio of n1 to n2 exceeds 1/3, indicating stability. Moreover, optimal stability and prolonged storage lifespan are achieved when the nano SiO_2 content is approximately 1.5%. This study contributes by synthesizing high-quality waterborne phenol-formaldehyde epoxy resin emulsions through optimized methods. The research findings offer a theoretical foundation for this domain and support the practical application of low-carbon and environmentally friendly concepts in the coatings industry.

KEYWORDS

waterborne phenolic-epoxy resin, emulsion preparation, nano SiO_2, high temperature resistance, low carbon, environmental protection

1 Introduction

1.1 Research background and significance

Amidst the escalating influence of global climate change, nations have implemented and progressively reinforced regulations and policies to constrain high-polluting and high-carbon industries, urging a shift towards low-carbon,

eco-friendly, and sustainable practices (Sovacool et al., 2022). Among these, the coatings industry, recognized as a significant polluter, confronts pressures from both regulatory mandates and market competition, compelling the development of products aligned with low-carbon and environmental standards to meet market demands (Pathak et al., 2022; Pleshivtseva et al., 2023).

Waterborne coatings, prized for their eco-friendly attributes, stand as a pivotal strategy for the coatings industry's pursuit of low-carbon transitions. Among these, waterborne epoxy resin emulsions, serving as pivotal constituents for various functional coatings, have garnered considerable scholarly and industrial focus in both production and application realms (Steinbrück et al., 2022). However, prevailing waterborne epoxy resin formulations often fall short of meeting demands for high-temperature conditions. Consequently, the development of waterborne epoxy resin emulsions capable of harmonizing low-carbon environmental performance with high-temperature resilience assumes critical importance, not only for advancing the low-carbon evolution of the coatings sector but also for presenting substantial industrial and market application opportunities in the realm of high-temperature-resistant materials utilizing waterborne epoxy resins. The significance of attaining a low-carbon footprint in the preparation process is twofold: it aligns with the global imperative to mitigate climate change and bolster environmental integrity, while also addressing the inherent need for sustainable growth within the coatings industry. Embracing low-carbon technologies and materials enables the industry to mitigate its environmental footprint, complying with stricter regulations and meeting evolving market expectations. Additionally, these technologies can bolster material performance and efficiency, fostering innovation in both materials and processes, thereby catalyzing the green transition and fostering high-quality development across the coatings industry worldwide.

This study begins by reviewing the current research landscape both domestically and internationally. It then outlines the main research methodologies employed, encompassing the preparation of waterborne phenol-formaldehyde epoxy resins, surface modification of nano silica (SiO_2), investigation into SiO_2-modified waterborne phenol-formaldehyde epoxy resin composites, and the *in situ* synthesis of nano SiO_2-modified waterborne phenol-formaldehyde epoxy resins. Subsequently, the prepared samples undergo testing, and the resultant findings are discussed. Ultimately, the research concludes by presenting its key findings and implications.

1.2 Research objectives

The primary research objectives of this study are outlined as follows:

(1) Synthesis of waterborne phenol-formaldehyde epoxy resin employing a phase transfer catalyst and a two-step alkaline method.
(2) Surface modification of nano SiO_2 utilizing γ-glycidoxypropyltriethoxysilane.
(3) Examination of the synthesis of SiO_2-modified waterborne phenol-formaldehyde epoxy resin composites through *in situ* polymerization, alongside the investigation of emulsion stability and coating performance.

TABLE 1 Information of experimental reagents.

Reagent name	Specification	Manufacturer
Phenol	Analysis pure	Aladdin
Formaldehyde	Analysis pure	Aladdin
Oxalic acid	Analysis pure	McLean
DEA	Analysis pure	McLean
Sodium p-aminobenzene sulfonate	Analysis pure	Aladdin
SDS	Analysis pure	McLean
Tetraethylammonium bromide	Analysis pure	Aladdin
Glacial acetic acid	Analysis pure	McLean
ECH	Analysis pure	Aladdin
ECH	Analysis pure	McLean
TETA		
Tetrahydrofuran	Analysis pure	McLean
Acetone	Analysis pure	Aladdin
Hydrochloric acid	Analysis pure	McLean
Sodium hydroxide	Analysis pure	Aladdin

TABLE 2 Details of experimental equipment.

Instrument name	Model	Manufacturer
High Shear Emulsifier	BME100LX	Brucker
Magnetic heating stirrer	DF-II	Hitachi
Nuclear magnetic resonance spectrometer	AVANCEIII500 MHz	Brucker
Fourier transform infrared spectrometer	TENSOR27	Brucker
Scanning electron microscope (SEM)	Zeiss_Supra55	Hitachi
Transmission electron microscope	JEM-2100	Hitachi
Thermogravimetric/ Differential thermal simultaneous analyzer	TGA/SDTA851e	Mettler Toledo
Pencil hardness tester	QHQ	Mettler Toledo
Particle size analyzer	ZetasizerNanoZS90	Malvern

2 Literature review

Numerous scholars have made significant progress in optimizing the preparation of waterborne phenol-formaldehyde epoxy resin. Wang H. et al. (2022) proposed a direct emulsification method using high-speed shearing and a large emulsifier to convert epoxy resin into emulsions. However, the resulting emulsion had a larger particle size and poor storage stability (Wang L. et al., 2022). In contrast, Aksoy (2022) highlighted the effectiveness of the phase inversion method in producing smaller and more stable emulsion products. This approach involves forming a water-soluble anionic intermediate by reacting epoxy resin with amine solvent, followed by adjusting the system's water acidity/alkalinity to induce the inversion of the anionic intermediate. It is considered more suitable for industrial production (Aksoy, 2022). Clark et al. (2022) demonstrated that existing waterborne epoxy resin products were most suitable for room temperature conditions but exhibited reduced adhesion, decreased hardness, and expansion phenomena at high temperatures, limiting their application in high-temperature industrial fields (Clark et al., 2022). Tang et al. (2022) suggested enhancing the high-temperature resistance of epoxy resin by selecting high-performance curing agents and reinforcing fillers, and optimizing the curing process and mechanisms. For instance, curing agents like polyurethane and phenolic resins could achieve curing at temperatures ranging from 120°C to 180°C (Tang et al., 2022). Ajanovic et al. (2022) devised a method to prepare a high-temperature-resistant waterborne phenol-formaldehyde epoxy resin emulsion, demonstrating superior thermal stability and solvent resistance. Through adjustments in parameters such as the content of phenol-formaldehyde resin, epoxy resin, and surfactant, as well as the type and dosage of surfactant under varying conditions, they achieved optimal emulsion performance (Ajanovic et al., 2022). Wang H. et al. (2022) highlighted that by controlling parameters like pH value, temperature, and stirring speed, along with specific conditions of phenol-formaldehyde resin content, epoxy resin content, and surfactant dosage, a more stable emulsion with enhanced performance could be obtained (Wang L. et al., 2022). Basak et al. (2024) developed novel nitrogen oxide-based nanogels using controlled reversible addition-fragmentation chain transfer polymerization, resulting in an over 85% increase in shelf life compared to natural superoxide dismutase (Basak et al., 2024). Das et al. (2018) evaluated these nanoparticles using techniques such as X-ray diffraction and Fourier Transform Infrared Spectroscopy (FTIR). They observed UV-visible spectra supporting the production of AgNPs on the surface of polydopamine-coated hydrated silica (SiO_2) (Das et al., 2018).

In conclusion, incorporating resins and curing agents with superior high-temperature adaptability into the curing system and optimizing synthesis and curing processes can synergistically enhance the high-temperature resistance and low-carbon performance of waterborne epoxy resin products.

3 Research method

Phenol-formaldehyde epoxy resin contains significant amounts of organic solvents, emitting large quantities of volatile organic compounds into the air after use. This fails to meet current environmental standards amidst low-carbon requirements, leading to increasingly restricted applications. Waterborne transformation of phenol-formaldehyde epoxy resin emerges as an effective solution. Given the higher epoxy value of phenol-formaldehyde epoxy resin compared to traditional epoxy resin, the introduction of hydrophilic groups can be achieved by reacting a portion of the epoxy groups, without compromising the comprehensive performance of the cured film. The specific research and preparation process are detailed below. The purities of the materials used in the experiment are as follows: phenol, 98%; formaldehyde, 34%; epichlorohydrin (ECH), 99%; tetrabutylammonium bromide, 98%; diethanolamine (DEA), 99%; and sodium p-toluenesulfonate, 98%.

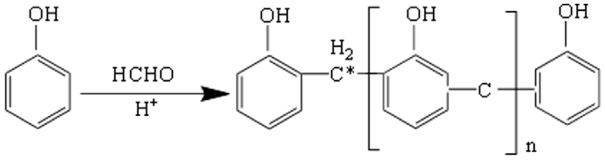

FIGURE 1
Preparation principle of phenolic resin.

3.1 Preparation of waterborne phenolic epoxy resin

The experiments involve various reagents. Table 1 presents the information for all reagents used in this experiment.

The instruments utilized in the experiments are outlined in Table 2.

The reagents and equipment utilized in this study are outlined previously. Next, the synthesis process of waterborne phenol-formaldehyde epoxy resin is elucidated. In a four-necked flask equipped with a condenser, 20.00 g of phenol, 3.00 g of deionized water, and 0.24 g of oxalic acid were added under an N2 atmosphere. The mixture is stirred magnetically at 60°C for 15 min, followed by the dropwise addition of 14.00 g of formaldehyde solution. After the completion of the addition, another 0.24 g of oxalic acid is added, and the temperature is raised to 75°C for a 2-h reaction. Subsequently, the temperature is further increased to 90°C, and the reaction continued for 2 h (Liu et al., 2022; Ma et al., 2022; Oyebanji et al., 2022). Following the reaction, the product is washed with water to neutrality and subjected to vacuum distillation to remove water, yielding the phenol-formaldehyde resin (I). The principle of this reaction is illustrated in Figure 1.

Under an N2 atmosphere, an excess of ECH and 0.48 g of tetra-n-butylammonium bromide (TBAB) is added to the previously obtained compound (I). The reaction temperature is set at 90°C for 3 h. Subsequently, the temperature is reduced to 70°C, and a sodium hydroxide (NaOH) solution is added dropwise, followed by an additional 2-h reaction period. Upon completion of the reaction, the product is washed with water to neutrality and subjected to vacuum distillation to remove the solvent. Finally, epoxy phenol novolac (EPN) (II) is obtained (Cohen et al., 2022; Wangari et al., 2022; Abdurahmonov et al., 2023). The principle of this reaction is illustrated in Figure 2.

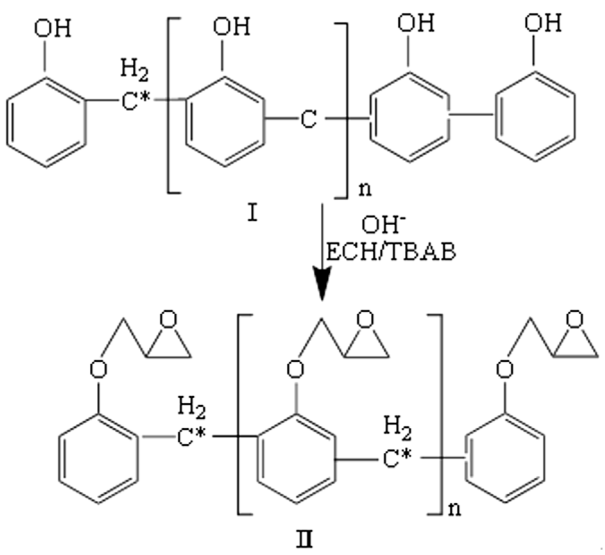

FIGURE 2
Preparation principle of EPN.

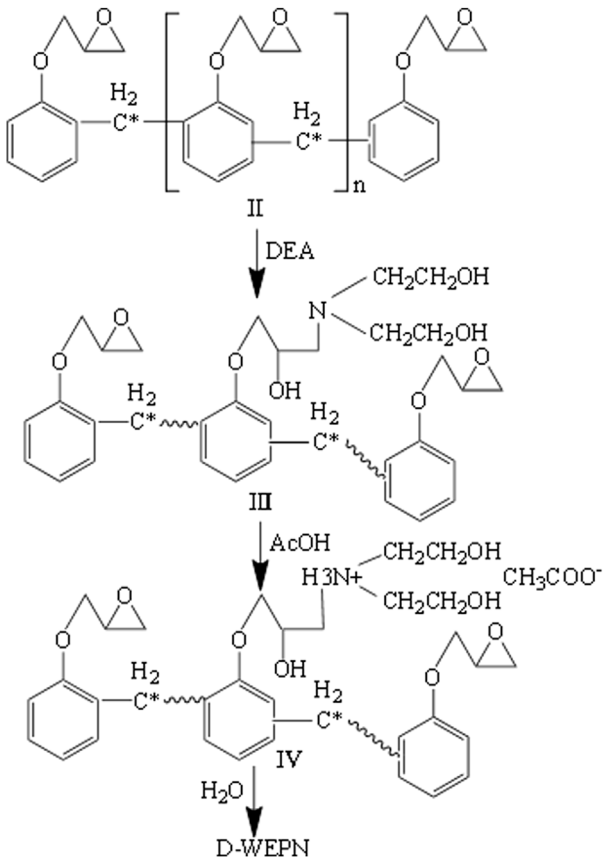

FIGURE 3
Preparation principle of D-WEPN.

TABLE 3 Information of characterization equipment.

Equipment	Function
Differential Scanning Calorimeter	Determines the thermal stability and glass transition temperature of materials. Provides crucial information about changes in thermal properties during heating for assessing application performance at high temperatures. |
Thermogravimetric analyzer	Measures mass changes of materials under heating or constant temperature conditions. Evaluates thermal stability and decomposition temperature, crucial for judging material suitability for high-temperature applications
Dynamic mechanical analyzer	Measures mechanical properties of materials under dynamic stress, including modulus (stiffness) and damping (energy dissipation). Obtains viscoelastic properties for understanding material performance at different temperatures
FTIR	Analyzes chemical bonds in materials, identifying infrared absorption peaks of specific chemical groups to understand chemical structure and possible cross-linking
SEM	Observes microstructure and morphology of materials. Analyzes surface and cross-section to evaluate dispersion of nano-fillers, compatibility, and influence of microstructure on material properties

A specified quantity of EPN (II) is dissolved in tetrahydrofuran (THF) at 65°C with stirring. DEA is then added according to the prescribed amount, and the reaction proceeded for a specific duration. Upon completion of the reaction, oxalic acid is introduced to neutralize the system for 0.5 h, followed by a temperature reduction to 55°C. Deionized water is subsequently slowly added while stirring for 1 h to yield the waterborne phenol-formaldehyde epoxy resin emulsion. This emulsion is labeled Diethanolamine Water Epoxy Phenol Novolac (D-WEPN) (Sun et al., 2022). The preparation principle of this emulsion is depicted in Figure 3.

3.1.1 Synthesis of anionic waterborne phenol-formaldehyde epoxy resin

EPN (II) is dissolved in THF at 65°C. Sodium p-amino benzenesulfonate is then added as per the specified amount, and the reaction proceeds at 100°C for 24 h (Wu et al., 2022). Subsequently, the temperature is reduced to 65°C, and the cosolvent sodium dodecyl sulfate (SDS) is introduced. Deionized water is slowly added dropwise while stirring for 2 h (Strassburger et al., 2023). Finally, high-shear emulsification is employed to form the emulsion, resulting in the waterborne phenol-formaldehyde epoxy resin emulsion denoted as S-WEPN.

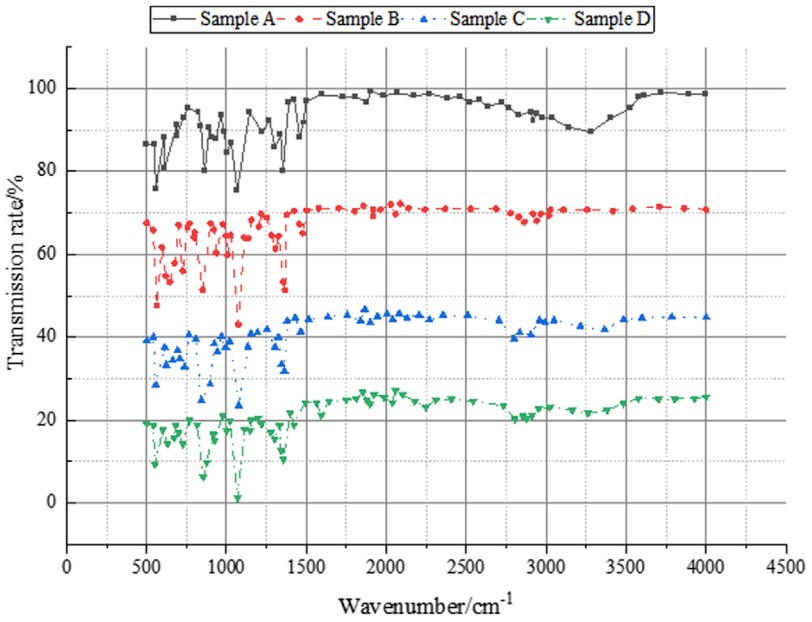

FIGURE 4
Results of the infrared test and analysis of conducted on the waterborne novolak epoxy resin.

3.1.2 Preparation of WEPN film

The prepared emulsion is combined with a defoaming agent and then applied onto a polytetrafluoroethylene template. Triethylenetetramine (TETA) curing agent is uniformly added and stirred. Vacuum curing is conducted at 50°C for 4 h, followed by additional curing at 110°C for 10 h, yielding the WEPN film (Hanif et al., 2023).

3.2 Nano SiO_2 surface modification and SiO_2 modified water-based phenolic epoxy resin composites

Nano SiO_2 undergoes surface modification using γ-aminopropyltriethoxysilane (APTES) to decrease surface hydroxyl (-OH) content and graft organic groups, thereby improving its hydrophobicity for enhanced dispersion in the resin (Gonçalves et al., 2022a; Kyei et al., 2022; Sonnendecker et al., 2022). More efficient surface modification is achieved by finely controlling the dosage of APTES and adjusting reaction conditions such as time and temperature. This results in a reduction of the hydroxyl content on the surface of nano SiO_2, thereby enhancing its dispersibility and hydrophobicity in phenolic epoxy resin, consequently improving the resin's high-temperature resistance. Subsequently, employing phenol-formaldehyde prepolymer, ECH, DEA, and acetic acid as primary constituents, the nanoscale SiO_2-modified waterborne phenol-formaldehyde epoxy resin is synthesized via the prepolymer method (Sharmila et al., 2022; Romão et al., 2022).

3.2.1 Experimental reagents and instruments

The experiment utilizes reagents listed in Table 1 and instruments detailed in Table 2.

3.2.2 Surface modification of nanoscale SiO_2

Initially, 4 g of nanoscale SiO_2 are dispersed in 100 mL of ethanol and stirred for 20 min, then sonicated for 30 min (Grinins et al., 2022; Henn et al., 2022; Vázquez Loureiro et al., 2023). Subsequently, 1.6 g of 3-APTES are dissolved in a 10-mL ethanol-water solution and stirred for 30 min for adequate hydrolysis. The dispersed mixture is then magnetically stirred at 70°C under a nitrogen atmosphere for 1 h, followed by the slow addition of APTES hydrolysate and an 8-h reaction (Wang H. et al., 2022; Koch et al., 2022; Thakare et al., 2022). Upon completion, centrifugation, washing with deionized water and ethanol, and centrifugation are conducted three times. Finally, vacuum drying is performed at 60°C for 24 h, succeeded by grinding and pulverization (Pan et al., 2022).

3.2.3 Synthesis of SiO_2/WEPN emulsion

Initially, under a nitrogen atmosphere, 20.00 g of phenol, 3.00 g of deionized water, and 0.24 g of oxalic acid are combined in a four-neck flask and magnetically stirred at 60°C for 15 min (Dagdag et al., 2022). Subsequently, 14 g of formaldehyde is added dropwise, followed by the introduction of 0.24 g of oxalic acid. The temperature is raised to 70°C, and the reaction proceeds for 2 h to yield the phenol-formaldehyde prepolymer. Then, N-SiO_2 is introduced, and the temperature was raised to 80°C for 2 h, followed by an additional 1 h of reaction at 95°C (Fritz and Olivera, 2022). Following neutralization through water washing, the system undergoes constant pressure fractionation, with water evaporated to obtain the nanoscale SiO2-modified phenol-formaldehyde resin. Excess ECH and 0.48 g of TBAB are added, and the reaction is conducted at 90°C for 3 h. Then, the temperature is lowered to 70°C, and a sodium hydroxide (NaOH) solution is added dropwise for a further 2 h. Subsequently, excess ECH and 0.48 g of TBAB are

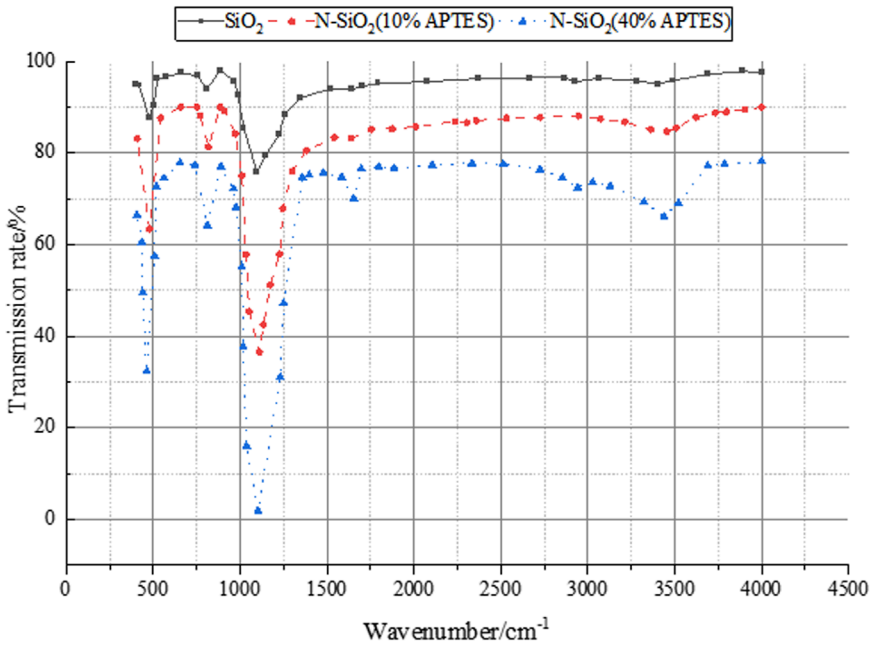

FIGURE 5
Infrared test and analysis results before and after nano SiO_2 modification.

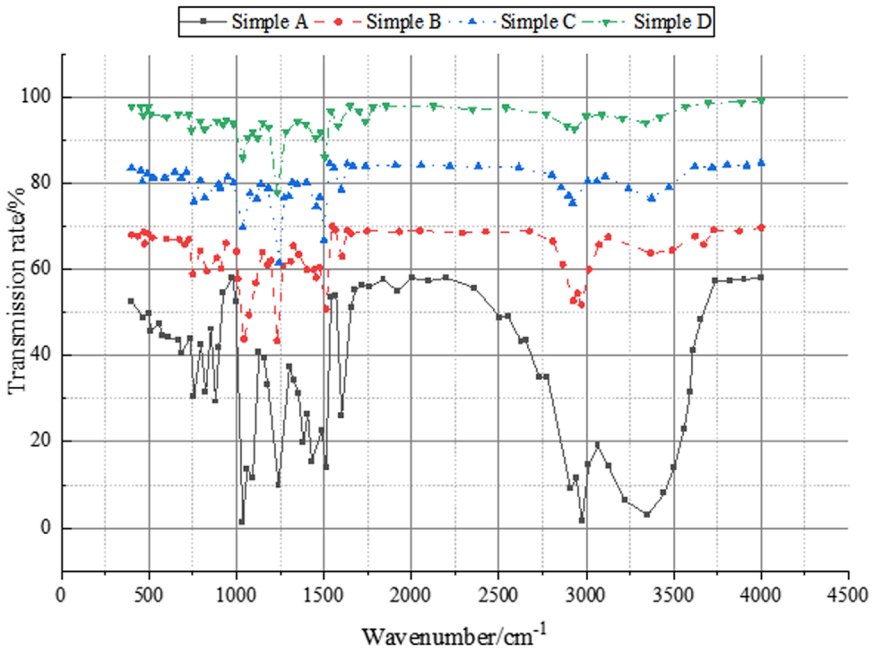

FIGURE 6
Analysis results of the infrared test conducted on nano SiO_2-modified waterborne novolac epoxy resin.

TABLE 4 Effect data of DEA dosage on average particle size and Zeta potential of emulsion.

n_1/n_2	1/4.5	1/4	1/3.5	1/3.25	1/3	1/2.5
Particle size (nm)	3500	2500	1300	1000	400	300
Zetapotential (mV)	18	20	22	24	32	35

TABLE 5 Detailed impact of DEA dosage on emulsion stability.

n_1/n_2	Centrifugal layering time/min	Emulsion appearance	Storage time/m
1/4.5	-	Light yellow with sediment	-
1/4	-	Light yellow with sediment	-
1/3.5	8	The milky white little precipitate	1
1/3.25	15	Milky white without precipitation	2
1/3	30	Milky white	More than 5
1/2.5	35	Milky white	More than 6

TABLE 6 Detailed impact of nano SiO_2 on emulsion stability.

N-SiO_2 addition amount	Appearance	Average particle size/nm	Centrifugal stability/min	Storage time/m
0	Milky white	326	30	More than 5
1.0	White transparent	375	30	More than 5
1.5	White transparent	430	25	More than 4
2.0	White transparent	415	25	More than 4
2.5	Light yellow transparent	690	20	3
3.0	Light yellow	887	20	3
3.5	Light yellow	1311	18	Less than 3

TABLE 7 Detailed impact of nano SiO_2 on the stability of modified water-based phenolic epoxy resin emulsion.

Content of SiO_2/%	0.0	0.5	1.0	1.5	2.0	2.5	3.0
Particle size (nm)	300	400	500	750	1000	1600	2000
Zetapotential (mV)	32	31.5	31.2	30.5	29	28	25

added, and the reaction is carried out at 90°C for 3 h. The temperature is then lowered again to 70°C, and NaOH solution is added dropwise to continue the reaction for 2 h (Gonçalves et al., 2022b; Okamura et al., 2022; Liang et al., 2023). After washing to neutral pH, the mixture undergoes constant pressure filtration and rotary evaporation to remove the solvents, resulting in SiO_2/EPN composite. The SiO_2/EPN is mixed with THF and stirred at 65°C until fully dissolved. DEA is added according to the stoichiometric ratio and reacted at 65°C for 2 h (Khan et al., 2022). Then, oxalic acid is added for neutralization and stirred for 1 h. The temperature is lowered to 55°C, and deionized water is added with stirring until a milky white system is formed, resulting in the SiO_2/WEPN emulsion.

3.2.4 Preparation of SiO_2/WEPN coating

The SiO_2-modified phenolic epoxy resin water-based emulsion is mixed with a defoaming agent and uniformly dripped into a polytetrafluoroethylene mold. The curing agent is added and stirred until homogeneous, followed by vacuum drying at 50°C for 4 h (Shibata et al., 2022). Subsequently, it is heat-cured at 110°C for 8 h to obtain the final SiO_2-modified phenolic epoxy resin composite coating.

3.3 *In-situ* synthesis of nano SiO_2-modified water-based phenolic epoxy resin

To achieve uniform dispersion of nano SiO_2 in the phenolic epoxy resin, this study employs an *in situ* polymerization method (Wen et al., 2022). The surface hydroxyl groups of nano SiO_2 are copolymerized with monomeric phenolic compounds and formaldehyde to obtain SiO_2-modified phenolic resin. Subsequently, it is further reacted with ECH, DEA, and acetic acid to produce a SiO_2-modified phenolic epoxy resin water-based emulsion (Steinbrück et al., 2022).

3.3.1 Experimental reagents and instruments

The reagents utilized in this experiment are detailed in Table 1, while the instruments employed are delineated in Table 2.

3.3.2 Synthesis of SiO_2/WEPN emulsion

Polyphenol is blended with nano SiO_2 and sonicated for 0.5 h to ensure uniform dispersion. Under a nitrogen atmosphere, formaldehyde is gradually added while maintaining a pH of 1–3 using oxalic acid, and the reaction proceeds at 65°C for 1 h. Subsequently, the temperature is raised to 85°C over 2 h, followed by an additional 2-h reaction to obtain SiO_2-modified phenolic resin (Mfune and Adams, 2022). Adequate epichlorohydrin is introduced, and at 85°C, the pH is adjusted to 8 using tetrabutylammonium bromide, with the reaction continuing for 2 h. The temperature is then reduced to 65°C, and the pH is stabilized using NaOH solution for an additional 2 h to yield SiO_2-modified phenolic epoxy resin. After water washing, the rotary evaporation process removes solvents and unreacted materials, resulting in the production of SiO_2-modified phenolic epoxy resin.

The prepared SiO_2-EPN is blended with THF and stirred at 65°C until completely dissolved. DEA is then added according to the stoichiometric ratio and allows to react for 2 h. Subsequently, oxalic acid is introduced for neutralization and reacted for 0.5 h. The gradual addition of deionized water with stirring for 1 h leads to the formation of the SiO_2/WEPN emulsion.

During the alkalization and etherification reactions, precise adjustments are made to the reaction conditions, optimizing the introduction of hydrophilic groups through the selection of appropriate phase transfer catalysts (TBAB) and modifiers (DEA and sodium p-aminobenzenesulfonate). This optimization results in waterborne phenolic epoxy resin emulsions with enhanced stability and high-temperature resistance. Furthermore, in the preparation of composite materials by incorporating modified nano SiO_2, a more uniform dispersion of nano SiO_2 is achieved through adjustments in the amount of SiO_2 added, dispersion method, and reaction conditions of the prepolymers. This not only improves the mechanical properties and chemical stability of the materials but also significantly enhances their high-temperature resistance. Details of the characterization equipment used in the experimental process are provided in Table 3.

4 Results and discussion

4.1 Infrared test and results

The prepared samples undergoes testing, including infrared analysis, emulsion stability assessment, and film performance evaluation. Following the removal of solvent from the samples, a FTIR test is conducted with a scanning range of 4000 to 500 cm^{-1}, 32 scans per sample, and a resolution of 4.0 cm^{-1}. Figure 4 depicts the analysis results of the waterborne novolak epoxy resin.

In Figure 4, the phenolic resin reveals numerous phenolic hydroxyl groups, evident through a broad absorption peak near 3300 cm^{-1} and characteristic benzene ring peaks at 1500–1600 cm^{-1}. Upon addition of epichlorohydrin, a distinctive epoxy peak emerges at 912 cm^{-1}, and most hydroxyl peaks near 3300 cm^{-1} diminish, indicating the completion of the epoxy reaction and the substitution of most hydroxyl groups by epoxy groups. Subsequent addition of DEA leads to some epoxy groups undergoing addition reactions to form hydroxyl groups, resulting in a weakened epoxy peak at 912 cm^{-1} and a strengthened hydroxyl peak near 3300 cm^{-1}. Neutralization with acetic acid yields a carboxyl carbonyl peak at 1734 cm^{-1}. Infrared spectroscopic analysis confirms the successful synthesis of phenolic epoxy resin, with the obtained product exhibiting the expected structure. Figure 5 presents the infrared test analysis results of nano SiO_2 modification before and after.

In Figure 5, the spectra reveal characteristic peaks of nano SiO_2 at 3435 cm^{-1}, 1105 cm^{-1}, 808 cm^{-1}, and 471 cm^{-1}. The peak at 3435 cm^{-1} corresponds to the absorption of hydroxyl groups (-OH) on the surface of SiO_2. The peak at 1105 cm^{-1} signifies the symmetric stretching vibration of Si-O-Si, while the peak at 808 cm^{-1} represents the antisymmetric stretching vibration of Si-O-Si. Additionally, the peak at 471 cm^{-1} corresponds to the bending vibration of Si-O-Si. Comparatively, the other two curves exhibit absorption peaks attributed to -CH_2 and -CH_3 groups near 2900 cm^{-1}, with the third peak being more prominent, indicating the introduction of -CH_2 and -CH_3 groups from 3-APTES. The enhancement of peaks near 1100 cm^{-1}, 800 cm^{-1}, and 470 cm^{-1} suggests the formation of Si-O-Si bonds. The broadening of the peak around 3400 cm^{-1} is attributed to the overlap between the -NH2 groups introduced by 3-APTES and the -OH groups.

Figure 6 depicts a comprehensive analysis of the infrared test results for the nano SiO_2-modified water-based phenolic epoxy resin.

In Figure 6, the Simple A curve reveals the presence of abundant phenolic hydroxyl groups in the phenolic resin, evidenced by the prominent and broad hydroxyl peak at 3400 cm^{-1}. Following the reaction with ECH, depicted in the Simple B curve, the hydroxyl groups undergo epoxidation, leading to a notable decrease in the hydroxyl peak at 3400 cm^{-1} and the emergence of an epoxy peak at 910 cm^{-1}. These data affirm the successful reaction between ECH and hydroxyl groups, evidenced by the attenuation of the hydroxyl peak. Upon the addition of DEA, depicted in the Simple C curve, some epoxy groups react with DEA to form hydroxyl groups, resulting in a reduction of the epoxy peak at 910 cm^{-1} and an augmentation of the hydroxyl peak at 3400 cm^{-1}. After neutralization with acetic acid, the Simple D curve reveals a

10.3389/fmats.2024.1406583

carboxyl carbonyl peak at 1732 cm^{-1}. Throughout the process, a faint Si-O-Si bending vibration peak at 471 cm^{-1} persists, indicating the formation of chemical bonds between SiO_2 and the EPN molecular chain.

4.2 Emulsion stability testing and results

Emulsion stability testing encompasses the assessment of various aspects, including the influence of DEA on the stability of the water-based phenolic epoxy resin emulsion, the impact of nano SiO_2 on the stability of SiO_2/WEPN composite material emulsion, and the effect of nano SiO_2 on the stability of modified water-based phenolic epoxy resin emulsion. The specific test results are outlined below, with detailed data on the impact of DEA dosage on the average particle size and zeta potential of the emulsion provided in Table 4.

When the ratio of n_1/n_2 exceeds 1/3, the absolute value of the system's zeta potential surpasses 32 mV, indicating high emulsion stability. With increasing DEA dosage, the emulsion particle size gradually decreases. However, when the n_1/n_2 ratio falls below 1/3.5, the particle size exceeds 1265 nm, signifying instability, possibly leading to gel formation. Within the range of 1/3.25 to 1/3, the emulsion particle size ranges from 324 to 859 nm, indicating moderate particle size conducive to stable storage. A n_1/n_2 ratio exceeding 1/3 results in particle size below 324 nm, signifying stable emulsion. Table 5 provides detailed insights into the impact of DEA dosage on emulsion stability.

As DEA dosage increases, the emulsion transitions from a pale yellow hue to milky white, and precipitate particles diminish. When the n_1/n_2 is ratio is ≤1/3.5, precipitation occurs, rendering the emulsion unstable. Conversely, with a n_1/n_2 ratio ≥1/3.25, minimal precipitation is observed, ensuring stable storage.

In Table 6, when the nano SiO_2 content exceeds 2%, the centrifugation time of the emulsion decreases rapidly due to nano SiO_2 aggregation. Consequently, the emulsion color gradually shifts to pale yellow, and stability decreases, resulting in shortened storage life, rendering it impractical. Based on dispersion and emulsion stability analyses, a nano SiO_2 content below 3% is optimal, with a recommendation of 2%.

In Table 7, when the nano SiO_2 content is below 2%, the absolute value of the Zeta potential exceeds 30 mV, indicating good system stability. However, as the nano SiO_2 content increases, the average particle size of the emulsion gradually increases. Once the nano SiO_2 content surpasses 2%, the average particle size of the emulsion exceeds 1000 nm, resulting in instability and the formation of precipitate particles. Therefore, it is advisable to maintain the nano SiO_2 content below 2%, ideally around 1.5%.

4.3 Coating film performance test

Table 8 displays the impact of nano SiO_2 content on various application properties of the coating films.

Table 8 displays the variation in coating properties with increasing nano SiO_2 content. Initially, the acid and alkali resistance

TABLE 8 Effect of nano SiO_2 content on other application properties of the coating film.

N-SiO_2	Acid resistance	Alkali resistance	Hardness	Impact resistance	Adhesion	Surface drying time/h	Solid drying time/h
0	Wrinkle and peel off	White and blistering	2	40	0	3	15
0.5	White and wrinkled	White and wrinkled	2	42	0	3	14
1.0	No change	White	3	45	0	3	14
1.5	No change	No change	3	50	0	2	13
2.0	No change	No change	3	50	1	2	13
2.5	Wrinkle	No change	3	50	1	2	12
3.0	White	No change	3	45	1	2	12

of the coatings rises before declining. Similarly, the impact resistance increases from 40 cm to 50 cm, then declines. Pencil hardness gradually elevates to 3H, while adhesion grade decreases from 0 to 1. Additionally, both surface and bulk drying times gradually decrease.

In Figure 6, the phenolic resin exhibits numerous phenolic hydroxyl groups, evident from the prominent and broad peak at 3400 cm^{-1} in the Simple A curve. Upon reaction with ECH, the hydroxyl groups undergo epoxidation, leading to a notable decrease in the hydroxyl peak at 3400 cm^{-1} and the emergence of an epoxy peak at 910 cm^{-1} in the Simple B curve. These data signify the effective reaction of ECH with hydroxyl groups and the attenuation of the hydroxyl peak. With the addition of DEA, some epoxy groups undergo an addition reaction with DEA, forming hydroxyl groups. This results in a reduction of the epoxy peak at 910 cm^{-1} and an amplification of the hydroxyl peak at 3400 cm^{-1} in the Simple C curve. Following neutralization with acetic acid, the Simple D curve displays a carboxyl carbonyl peak at 1732 cm^{-1}. Notably, a weak Si-O-Si bending vibration peak at 471 cm^{-1} persists throughout the process, indicating chemical bonding between SiO_2 and the EPN molecular chain.

The enhanced water-based phenolic epoxy resin emulsion, distinguished by its remarkable high-temperature resistance, chemical stability, environmental compatibility, and superior mechanical attributes, holds immense promise across various applications. It finds suitability in surface coatings within sectors such as automotive, aerospace, and industrial machinery, offering enduring corrosion protection. Moreover, serving as a matrix resin, it augments material high-temperature performance, making it ideal for high-performance composite materials fabrication. Additionally, it meets the requirements for high-strength bonding in elevated-temperature environments, applicable in industrial equipment and aerospace component bonding. In contrast to the research endeavors of others, exemplified by Pan and Yan (2023), focusing predominantly on enhancing high-temperature resistance through alterations in resin cross-linking density, this study fortifies high-temperature resistance via optimized preparation processes, nano SiO_2 surface modification, and composite material techniques. This approach not only elevates high-temperature resistance but also ensures environmental compatibility and widens application horizons (Pan and Yan, 2023). Similarly, juxtaposed with the research conducted by Zhao et al. (2022), which concentrates on leveraging diverse chemical modification methods to bolster resin physical properties, this study, through comprehensive methodological optimization, not only achieves enhancements in physical attributes but also broadens material application realms by incorporating nano-fillers, particularly in demanding high-temperature and high-performance sectors (Zhao et al., 2022).

5 Conclusion

This study aims to enhance phenolic epoxy resin by incorporating nano SiO_2 to produce water-based phenolic epoxy resin, thus achieving water-based properties and augmenting its high-temperature resistance. Furthermore, the adoption of water-based phenolic epoxy resin aids in reducing volatile emissions, aligning with the environmental requisites of a low-carbon context. The specific research conclusions are delineated as follows:

(1) The synthesis of phenolic epoxy resin proceeds smoothly, with the replacement of hydroxyl groups by epoxy groups. Some epoxy groups react with DEA to yield hydroxyl groups.
(2) The characteristic spectral peaks of nano SiO_2 are attributed to the vibration of Si-O-Si bonds. Introduction of 3-APTES enhances the vibration peak of Si-O-Si bonds.
(3) Upon reaction with ECH, hydroxyl groups in the phenolic resin are epoxidized. Following DEA addition, some epoxy groups react with DEA to form hydroxyl groups. SiO_2 is chemically bonded to the EPN molecular chain.
(4) When the ratio of n1/n2 exceeds 1/3, with an absolute Zeta potential value surpassing 32 mV, the emulsion maintains stability. However, as DEA dosage increases, instability occurs when the ratio of n1/n2 falls below 1/3.5. Within the range of 1/3.25 to 1/3, the emulsion exhibits a moderate particle size, facilitating stable storage. A ratio of n1/n2 exceeding 1/3 signifies emulsion stability, with particle size below 324 nm.
(5) The emulsion transitions from pale yellow to milky white with rising DEA dosage. Instability and precipitation occur when the ratio of n1/n2 is ≤1/3.5, while stability prevails when the ratio is ≥1/3.25.
(6) Beyond a nano SiO_2 content of 2%, emulsion stability diminishes, leading to reduced storage life and an average particle size exceeding 1000 nm, resulting in precipitate particle formation. It is advisable to maintain nano SiO_2 content below 2%, ideally around 1.5%.

While this study yields promising outcomes, there are certain limitations to consider. It exclusively addresses the preparation of a singular type of phenolic epoxy resin emulsion, neglecting exploration into alternative phenolic epoxy resin emulsions. Future research endeavors will involve conducting more extensive application studies to assess the emulsion's performance in practical settings. Additionally, comparative analyses among various phenolic epoxy resin emulsions will be undertaken to ascertain the optimal choices.

Data availability statement

The original contributions presented in the study are included in the article/Supplementary material, further inquiries can be directed to the corresponding author.

Author contributions

YL: Conceptualization, Investigation, Writing–original draft, Writing–review and editing. JG: Conceptualization, Investigation, Writing–original draft, Writing–review and editing. JY: Data curation, Methodology, Writing–original draft. LW: Project

administration, Validation, Writing–review and editing. XW: Data curation, Project administration, Writing–original draft. XX: Conceptualization, Data curation, Investigation, Methodology, Writing–review and editing. FY: Software, Writing–review and editing. LH: Software, Writing–original draft, Writing–review and editing.

Funding

The author(s) declare that no financial support was received for the research, authorship, and/or publication of this article.

Acknowledgments

The authors would like to show sincere thanks to those techniques who have contributed to this research.

Conflict of interest

Authors YL, JY, LW, XW, XX, FY, and LH were employed by the Suzhou Paint-key Material Technology Co., Ltd.

The remaining author declares that the research was conducted in the absence of any commercial or financial relationships that could be construed as a potential conflict of interest.

Publisher's note

References

Abdurahmonov, A., Madamiovna, K. D., and Egamberdiyeva, T. (2023). High temperature resistant reinforced concrete made on the basis of industrial waste. *Best J. Innovation Sci. Res. Dev.* 2 (3), 26–33. doi:10.15407/scine16.02.051

Ajanovic, A., Sayer, M., and Haas, R. (2022). The economics and the environmental benignity of different colors of hydrogen. *Int. J. Hydrogen Energy* 47 (57), 24136–24154. doi:10.1016/j.ijhydene.2022.02.094

Aksoy, K. (2022). Water-based polyurethanes for antibacterial coatings: an overview. *Eur. J. Res. Dev.* 2 (4), 213–242. doi:10.56038/ejrnd.v2i4.124

Basak, S., Mukherjee, I., and Das, T. K. (2024). Injectable biocompatible raft mediated nitroxide nanogels: a robust ROS-reduction antioxidant approach. *Colloids Surfaces B Biointerfaces* 236, 113790. doi:10.1016/j.colsurfb.2024.113790

Clark, M., Springmann, M., Rayner, M., Scarborough, P., Hill, J., Tilman, D., et al. (2022). Estimating the environmental impacts of 57,000 food products. *Proc. Natl. Acad. Sci.* 119 (33), e2120584119. doi:10.1073/pnas.2120584119

Cohen, R., Eames, P. C., Hammond, G. P., Newborough, M., and Norton, B. (2022). Briefing: the 2021 Glasgow Climate Pact: steps on the transition pathway towards a low carbon world. *Proc. Institution Civ. Engineers-Energy, Int. J. Hydrogen Energy* 175 (3), 97–102. doi:10.1680/jener.22.00011

Dagdag, O., Hsissou, R., Safi, Z., Hamed, O., Jodeh, S., Haldhar, R., et al. (2022). Viscosity of epoxy resins based on aromatic diamines, glucose, bisphenolic and bio-based derivatives: a comprehensive review. *J. Polym. Res.* 29 (5), 200. doi:10.1007/s10965-022-03040-3

Das, T. K., Ganguly, S., Bhawal, P., Remanan, S., Ghosh, S., and Das, N. C. (2018). A facile green synthesis of silver nanoparticles decorated silica nanocomposites using mussel inspired polydopamine chemistry and assessment its catalytic activity. *J. Environ. Chem. Eng.* 6 (6), 6989–7001. doi:10.1016/j.jece.2018.10.067

Fritz, C., and Olivera, J. F. (2022). Nanocellulose in heterogeneous water-based polymerization for wood adhesives. *Polysaccharides* 3 (1), 219–235. doi:10.3390/polysaccharides3010012

Gonçalves, F. A., Santos, M., Cernadas, T., Alves, P., and Ferreira, P. (2022a). Influence of fillers on epoxy resins properties: a review. *J. Mater. Sci.* 57 (32), 15183–15212. doi:10.1007/s10853-022-07573-2

Gonçalves, F. A., Santos, M., Cernadas, T., Ferreira, P., and Alves, P. (2022b). Advances in the development of biobased epoxy resins: insight into more sustainable materials and future applications. *Int. Mater. Rev.* 67 (2), 119–149. doi:10.1080/09506608.2021.1915936

Grinins, J., Iesalnieks, M., Biziks, V., Gritane, I., and Sosins, G. (2022). Birch wood surface characterization after treatment with modified phenol-formaldehyde oligomers. *Polymers* 14 (4), 671. doi:10.3390/polym14040671

Hanif, Z., Choi, K. I., Jung, J. H., Pornea, A. G. M., Park, E., Cha, J., et al. (2023). Dispersion enhancement of boron nitride nanotubes in a wide range of solvents using plant polyphenol-based surface modification. *Industrial Eng. Chem. Res.* 62 (6), 2662–2670. doi:10.1021/acs.iecr.2c03897

Henn, K. A., Forssell, S., Pietiläinen, A., Forsman, N., Smal, I., Nousiainen, P., et al. (2022). Interfacial catalysis and lignin nanoparticles for strong fire-and water-resistant composite adhesives. *Green Chem.* 24 (17), 6487–6500. doi:10.1039/d2gc01637k

Khan, S. A. R., Godil, D. I., Yu, Z., Abbas, F., and Shamim, M. A. (2022). Adoption of renewable energy sources, low-carbon initiatives, and advanced logistical infrastructure-an step toward integrated global progress. *Sustain. Dev.* 30 (1), 275–288. doi:10.1002/sd.2243

Koch, S. M., Pillon, M., Keplinger, T., Dreimol, C. H., Weinkotz, S., and Burgert, I. (2022). Intercellular matrix infiltration improves the wet strength of delignified wood composites. *ACS Appl. Mater. Interfaces* 14 (27), 31216–31224. doi:10.1021/acsami.2c04014

Kyei, S. K., Eke, W. I., Darko, G., and Akaranta, O. (2022). Natural polyhydroxy resins in surface coatings: a review. *J. Coatings Technol. Res.* 19 (3), 775–794. doi:10.1007/s11998-021-00604-8

Liang, Y., Luo, Y., Wang, Y., Fei, T., Dai, L., Zhang, D., et al. (2023). Effects of lysine on the interfacial bonding of epoxy resin cross-linked soy-based wood adhesive. *Molecules* 28 (3), 1391. doi:10.3390/molecules28031391

Liu, X. J., Zheng, M. S., Chen, G., Dang, Z. M., and Zha, J. W. (2022). High-temperature polyimide dielectric materials for energy storage: theory, design, preparation and properties. *Energy & Environ. Sci.* 15 (1), 56–81. doi:10.1039/d1ee03186d

Ma, Y., Wan, J., Yang, Y., Ye, Y., Xiao, X., Boyle, D. T., et al. (2022). Scalable, ultrathin, and high-temperature-resistant solid polymer electrolytes for energy-dense lithium metal batteries. *Adv. Energy Mater.* 12 (15), 2103720. doi:10.1002/aenm.202103720

Mfune, P., and Adams, S. (2022). Spray-painters and occupational contact dermatitis. *Curr. Allergy & Clin. Immunol.* 35 (3), 164–168. doi:10.1016/j.ijhydene.2022.02.094

Okamura, N., Kimura, T., Harada, T., and Hashimoto, T. (2022). Water-based dispersions of luminescent metal complexes for wet-processed multilayer organic light-emitting diodes. *Mol. Cryst. Liq. Cryst.* 744 (1), 31–36. doi:10.1080/15421406.2022.2055257

Oyebanji, M. O., Castanho, R. A., Genc, S. Y., and Kirikkaleli, D. (2022). Patents on environmental technologies and environmental sustainability in Spain. *Sustainability* 14 (11), 6670. doi:10.3390/su14116670

Pan, P., and Yan, X. (2023). Preparation of antibacterial nanosilver solution microcapsules and their impact on the performance of Andoung wood surface coating. *Polymers* 15 (7), 1722. doi:10.3390/polym15071722

Pan, P., Yan, X., and Wang, L. (2022). Effects of thermochromic fluorane microcapsules and self-repairing waterborne acrylic microcapsules on the properties of water-based coatings on basswood surface. *Polymers* 14 (12), 2500. doi:10.3390/polym14122500

Pathak, T. K., Sharma, V., Jassal, P. S., Singh, R. P., and Johar, R. (2022). Bio-modified pyrotechnic composite materials for firefighting application. *Fire Mater.* 46 (8), 1168–1179. doi:10.1002/fam.3060

Pleshivtseva, Y., Derevyanov, M., Pimenov, A., and Rapoport, A. (2023). Comprehensive review of low carbon hydrogen projects towards the decarbonization pathway. *Int. J. Hydrogen Energy* 48 (10), 3703–3724. doi:10.1016/j.ijhydene.2022.10.209

Romão, E. G. M., Oliveira, M. P., and Guerrini, L. M. (2022). Evaluation of the oligomeric epoxy silane as coupling agent on thermal and mechanical

properties of water-based acrylate adhesives. *Polym. Eng. Sci.* 62 (10), 3310–3322. doi:10.1002/pen.26105

Sharmila, V. G., Tamilarasan, K., Kumar, M. D., Kumar, G., Varjani, S., Kumar, S. A., et al. (2022). Trends in dark biohydrogen production strategy and linkages with transition towards low carbon economy: an outlook, cost-effectiveness, bottlenecks and future scope. *Int. J. Hydrogen Energy* 47 (34), 15309–15332. doi:10.1016/j.ijhydene.2021.12.139

Shibata, A., Takeda, Y., Kimura, Y., and Tsuji, N. (2022). Hydrogen-related fracture behavior under constant loading tensile test in as-quenched low-carbon martensitic steel. *Metals* 12 (3), 440. doi:10.3390/met12030440

Sonnendecker, C., Oeser, J., Richter, P. K., Hille, P., Zhao, Z., Fischer, C., et al. (2022). Low carbon footprint recycling of post-consumer PET plastic with a metagenomic polyester hydrolase. *ChemSusChem* 15 (9), e202101062. doi:10.1002/cssc.202101062

Sovacool, B. K., Newell, P., Carley, S., and Fanzo, J. (2022). Equity, technological innovation and sustainable behaviour in a low-carbon future. *Nat. Hum. Behav.* 6 (3), 326–337. doi:10.1038/s41562-021-01257-8

Steinbrück, M., Stegmaier, U., Große, M., Czerniak, L., Lahoda, E., Daum, R., et al. (2022). High-temperature oxidation and quenching of chromium-coated zirconium alloy ATF cladding tubes with and w/o pre-damage. *J. Nucl. Mater.* 559 (15), 153470. doi:10.1016/j.jnucmat.2021.153470

Strassburger, D., Silveira, M. R., Baldissera, A. F., and Ferreira, C. A. (2023). Performance of different water-based resins in the formulation of intumescent coatings for passive fire protection. *J. Coatings Technol. Res.* 20 (1), 201–221. doi:10.1007/s11998-021-00597-4

Sun, L., Yang, J., and Yan, J. (2022). The structure and properties of water-based silicone blended phenolic resin and its application in oil filter paper-based materials. *Korean J. Chem. Eng.* 39 (8), 2201–2210. doi:10.1007/s11814-022-1073-8

Tang, Y. M., Chau, K. Y., Fatima, A., and Waqas, M. (2022). Industry 4.0 technology and circular economy practices: business management strategies for environmental sustainability. *Environ. Sci. Pollut. Res.* 29 (33), 49752–49769. doi:10.1007/s11356-022-19081-6

Thakare, D. R., Xiong, T. M., Flueck, I. L., Morado, E. G., Zimmerman, S. C., and Sottos, N. R. (2022). Acid-responsive anticorrosion microcapsules for self-protecting coatings. *Macromol. Chem. Phys.* 223 (5), 2100382. doi:10.1002/macp.202100382

Vázquez Loureiro, P., Lestido-Cardama, A., Sendón, R., Bustos, J., Paseiro Losada, P., and Rodríguez Bernaldo de Quirós, A. (2023). Identification of potential migrants from epoxy and organosol coatings used in metal food cans. *Food Addit. Contam. Part A* 40 (4), 597–611. doi:10.1080/19440049.2023.2183051

Wang, H., Li, X., Zhao, X., Li, C., Song, X., Zhang, P., et al. (2022a). A review on heterogeneous photocatalysis for environmental remediation: from semiconductors to modification strategies. *Chin. J. Catal.* 43 (2), 178–214. doi:10.1016/s1872-2067(21)63910-4

Wang, L., Chen, L., and Li, Y. (2022b). Digital economy and urban low-carbon sustainable development: the role of innovation factor mobility in China. *J. Nucl. Mater.* 29 (32), 48539–48557. doi:10.1007/s11356-022-19182-2

Wangari, T. N., Mahajan, G., and Chauhan, B. S. (2022). Glyphosate resistance in junglerice (Echinochloa colona) and alternative herbicide options for its effective control. *Weed Technol.* 36 (1), 38–47. doi:10.1017/wet.2021.100

Wen, Z., Chen, S., Li, A., Sun, M., Zhang, Y., and Wang, W. (2022). Anticorrosive performance of polyaniline/aluminum tripolyphosphate/waterborne epoxy composite coatings. *J. Adhesion Sci. Technol.* 36 (23-24), 2527–2546. doi:10.1080/01694243.2022.2067434

Wu, C., Pan, X., Lin, F., Cui, Z., Li, X., Chen, G., et al. (2022). High-temperature electrical properties of polymer-derived ceramic SiBCN thin films fabricated by direct writing. *Ceram. Int.* 48 (11), 15293–15302. doi:10.1016/j.ceramint.2022.02.063

Zhao, Y., Xiao, Z., Feng, Z., Luo, Q., Liu, X., and Cui, W. (2022). Super hydrophobic SiO2/phenolic resin-coated filter screen and its application in efficient oil–water separation. *Materials* 15 (23), 8395. doi:10.3390/ma15238395